Atmósfera (1998) 12, pp. 1-13

Characteristics of the atmospheric boundary layer for coastal and inland locations around the Gulf of Mexico

A. BIROL KARA and JAMES B. ELSNER

Department of Meteorology, The Florida State University, Tallahassee, FL, 32306-4520, USA

(Manuscript received Oct. 13, 1997; accepted in final form June 10, 1998)

RESUMEN

Este trabajo examina aspectos de la capa límite atmosférica (ABL) de varios lugares costeros y tierra adentro de los Estados Unidos que ven hacia el Golfo de México. Se llevan a cabo simulaciones usando el modelo de capa límite de la Oregon State University (OSU) bajo un evento de flujo regresado del Golfo de México. Para el análisis del modelo, las alturas ABL se obtienen usando valores de la humedad del suelo provenientes del modelo Eta. Las alturas ABL obtenidas de estos pronósticos de 24 hrs son entonces comparadas con otras formulaciones estándar. Se demuestra que pronósticos errados de las alturas de la ABL en el modelo, bajo condiciones muy estables, pueden evitarse usando una fórmula de interpolación. Los resultados confirman que la velocidad de fricción en la capa límite a lo largo de la costa del Golfo es pequeña.

Una relación fuerte entre la velocidad de fricción y la longitud Monin-Obukov en las localidades costeras es debida probablemente a flujos superficiales con relativamente escaso flujo térmico.

En los lugares costeros de Florida y Texas, la turbulencia mecánica produce grandes parámetros estructurales de temperatura en la superficie, ya que la velocidad del viento es comúnmente débil en los pronósticos del modelo.

ABSTRACT

This paper examines aspects of the atmospheric boundary layer (ABL) for several U. S. coastal and inland locations around the Gulf of Mexico. Simulations are performed using the Oregon State University (OSU) planetary boundary layer model under a Gulf of Mexico return-flow event. For the model analyses, the ABL heights are obtained using soil moisture values from the *Eta* model. The ABL heights obtained from these 24-hr forecasts are then compared with other standard formulations. It is shown poor forecasts of the ABL height in the model under very stable conditions can be prevented by using an interpolation formula. Results confirm that friction velocity in the boundary layer along the Gulf coast is small. A strong relationship between friction velocity and *Monin-Obukhov* length at coastal locations is likely due to surface fluxes with relatively unimportant heat flux. At coastal locations of Florida and Texas, mechanical turbulence causes large temperature structure parameter at the surface since wind speed is usually calm in the model forecasts.

1. Introduction

The main consequence of a so-called "return-flow event" is the large amount of moisture coming from Gulf to the coastal and inland locations in the U. S. The return-flow cycle begins as classic airmass modification when cold and dry continental air tracks over a relatively warm ocean (offshore flow), but it is distinguished from the classic modification process by synoptic conditions that cause the modified air to return to the land as an onshore flow (Crisp and Lewis, 1992). The northward transport of moisture from the Gulf of Mexico to coastal and inland locations associated with return-flow on the backside of a retreating surface anticyclone may cause some difficulty in forecasting ABL parameters, such as surface fluxes, especially in numerical models (Lewis and Crisp, 1992). Recently an air mass transformation model was developed to diagnose and predict weather events around the Gulf of Mexico (Kara *et al.*, 1998; Kara, 1996). Results from these studies suggest that improved predictions of return-flow events are possible during the cool season.

Several different approaches have been made to forecast boundary layer parameters such as, boundary layer depth, temperature, and stability (Businger and Arya, 1974; Troen and Mahrt, 1986). Good forecasts of ABL height are necessary for accurate forecasts of several ABL parameters, such as boundary layer clouds (Clarke, 1970; André and Mahrt, 1982). However, determination of ABL height is not easy and even more difficult for nighttime conditions. This was discussed in several modeling studies (Zhang and Anthes, 1982; Clarke and Hess, 1973). Troen and Mahrt (1986) forecast an ABL height based on the critical *Richardson number*, and in this formulation the transition between stable case and unstable case is continuous. However, the classic similarity theory for the nocturnal boundary layer leads to significant overestimation of surface cooling because of poor vertical resolution where turbulence may occur in thin layers even when the *Richardson number* over the model is large. As a result, the determination of ABL height during the night, especially under very stable conditions poses a few potential problems in the model.

The temperature structure parameter is another variable to examine for both coastal and inland locations since it is highly dependent on stability and wind speed. Observations indicated that the temperature structure parameter increases near the surface due to high shear of the horizontal winds, and it is small at the top of the boundary layer as shown in Cuijpers and Kohsiek (1988). They also noted that the structure parameter increases near the surface during nights with a calm geostrophic wind speed. The model of Sorbjan (1986) indicates that the greater the atmospheric stability, the larger the structure parameter even though observations do not necessarily show such behavior.

The present paper is an outgrowth of a study by Kara *et al.* (1998) which includes a complete description of model equations and computational procedures for the Oregon State University planetary boundary layer model (see also Mahrt and Pan 1984, Troen and Mahrt, 1986; Pan and Mahrt, 1987). Because the model is throughly explained in the literature, this paper deals solely with technical aspects of the boundary layer during a particular Gulf of Mexico return-flow event. During the event, characteristics of ABL are examined for several coastal and inland locations (Fig. 1), separately and comparisons are made between two regions. Coastal stations include Brownsville (BRO) and Corpus Christi (CRP), Texas, as well as Tallahassee (TLH), and Tampa Bay (TBW), Florida. The inland locations include Lake Charles (LCH), Louisiana, Jackson (JAN), Mississippi, and Shelby Co Airport (BMX), Alabama.

In this paper, details of the ABL height specification are provided in section 2 followed by a discussion of stability effects in predicting ABL height in section 3. In particular, the temperature structure parameter is examined in section 4. Summary and conclusions are given in section 5.

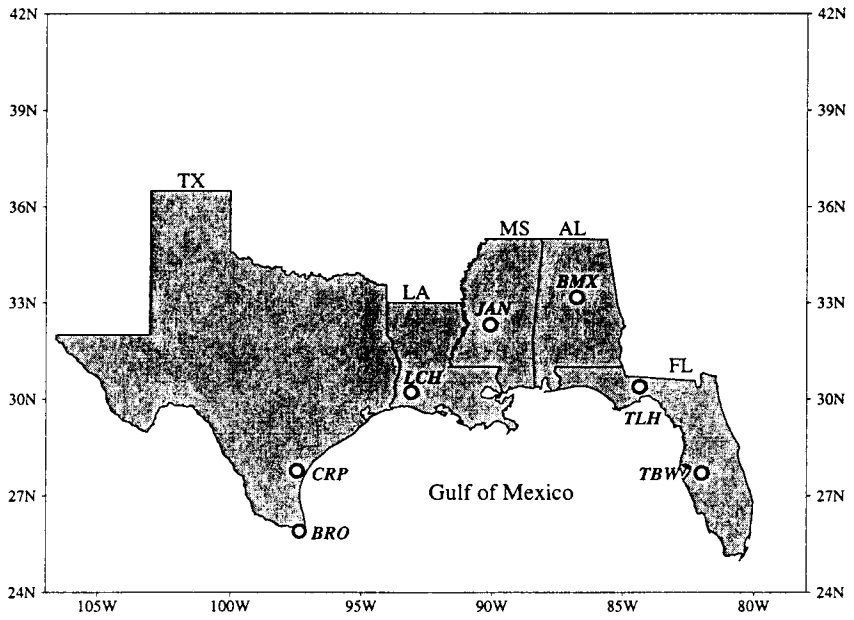

Fig. 1. The locations of coastal and inland stations around the Gulf of Mexico in Texas (TX), Louisiana (LA), Mississippi (MS), Alabama (AL), and Florida (FL) considered in this study.

2. ABL Height

The OSU model calculates ABL height (h) as follows:

$$h = \frac{Ri_{cr}\theta_{ov}|V(h)|^2}{g[\theta_v(h) - \theta^*_{ov}]} \tag{1}$$

where Ri_{cr} (nondimensional) is the critical *Richardson number* (0.25), θ_{ov} is the reference virtual potential temperature at the first model level above the surface, θ^*_{ov} is the low-level potential temperature (Troen and Mahrt, 1986), and g is the gravity acceleration (9.8 m s^{-2}).

Figure 2 shows model ABL height changes for both coastal and inland locations. Wind speed and directions for each station at the beginning of the model initialization, on 12 UTC Feb 8 and 24 hours later, are also shown. As expected, during the day, growth of the boundary layer is noted for all stations both along the coast and inland. Growth rate is the largest for TBW and LCH. After nightfall, a dramatic collapse is observed at all locations, with the exception of TLH where the model indicated a gradual lowering of the ABL height. With the exception of the Florida stations, a secondary nocturnal growth of the ABL height is also observed in the model. It should be noted that lightest wind speeds were observed in Florida coast. When the ABL collapsed at night, model wind speeds were approximately between 0.4-1.6 m s^{-1}. On the other hand, wind speeds were between 1.2-5.8 m s^{-1} when the ABL grew at night. Besides wind, another reason for these changes in the ABL height is soil moisture. The model is very sensitive to the exact specification of soil moisture (Troen and Mahrt, 1986). A detail analysis of soil moisture and soil types used for these coastal and inland locations are found in Kara *et al.* (1998).

ABL height calculations in the model are biased toward small values under very stable condi-

tions (Ruscher, 1988). The model uses a minimum value of 50 m even if Eq. 1 results in an ABL height of less than 50 m. Here we compare other ABL height formulations to the performance of the ABL height we obtained from the model during the return-flow cycle of February 2-9, 1996. The investigation is performed under various stability classifications (Clarke and Hess, 1973) as will be explained later. Specifically, an investigation is made here of the various diagnostic relationships that are indicated in the literature for the nocturnal ABL height. One common formula used for nocturnal ABL height determination is $H = c\frac{u_*}{f}$ where c is a constant, u_* is the friction velocity and f is the coriolis parameter. Several different values were suggested for c. For example, Koracin and Berkowicz (1988) used a value of $c = 0.07$ while Benkley and Schulman (1979) suggested a value of $c = 0.185$. This variability is attributed to differences in stability.

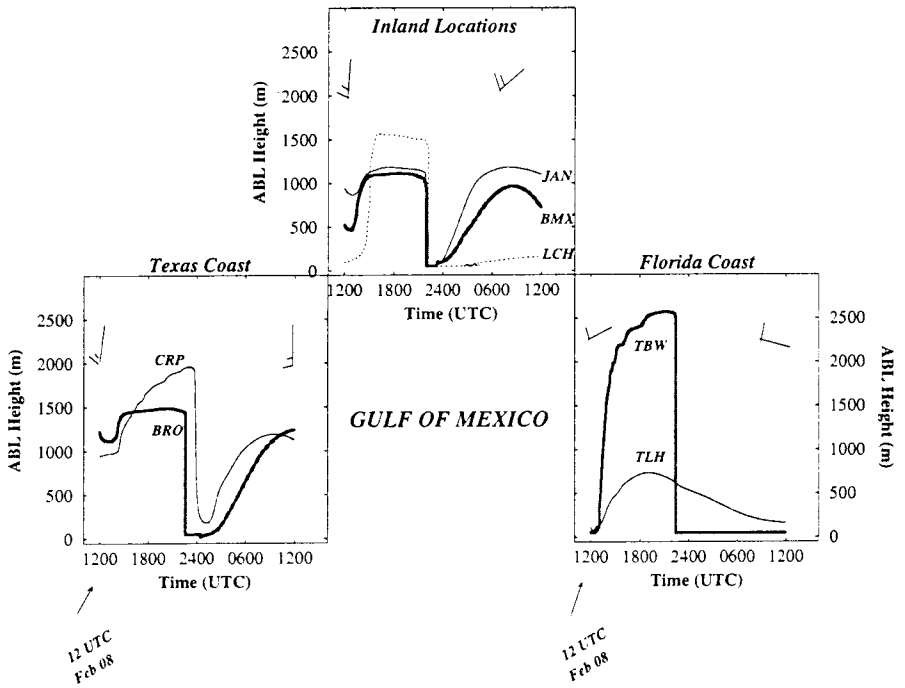

Fig. 2. ABL heights (for a 24-h period) during the onshore/return-flow phase of the return-flow cycle of Feb 2-9 for both inland and coastal stations.

Here nocturnal ABL heights obtained from the OSU model, for coastal and inland locations are compared with formulations of Businger and Arya (1974), Yu (1977) and Deardorff (1972) during the return-flow event of February 2-9. These formulations are as follows, respectively:

$$h_1 = \frac{k.u_*}{f}, \tag{2}$$

$$h_2 = \sqrt{\frac{k.u_*.L}{f}}, \tag{3}$$

$$h_3 = \frac{1}{\left(\frac{1}{30L} + \frac{f}{0.35u_*}\right)}, \tag{4}$$

where, L denotes *Monin-Obukhov* length. For comparisons, all four boundary layer heights (h, h_1, h_2 and h_3) were calculated each hour throughout the night. In addition, the dimensionless stability parameter, $\mu_* = \frac{k.u_*}{fL}$, was calculated for each hour, and stability classifications of the nocturnal boundary layer were prepared using the method of Clarke and Hess (1973). The calculations were made using a *von Kármán* constant (k) of 0.4 and a Coriolis parameter, $f = 2\Omega \sin\phi(\Omega = 7.292 \times 10^{-5}\ s^{-1})$, for each coastal and inland station since the calculations for three of the four ABL heights are quite sensitive to the Coriolis parameter (see Eqs. 2, 3, 4).

The purpose of these analyses is to examine under which stability conditions the OSU model performs well and to find which formulation of boundary layer height gives the best results for the actual ABL height; so that, a new formula can be adapted to the model when h is below 50 m. For this purpose, the performance of both coastal and inland stations have been examined separately to see the differences. The correlation coefficients (r) between ABL model height (h) and the others (h_1, h_2, h_3) for each category and for each stability classification are shown in Table 1.

The significance of the correlation coefficients was tested using the *student t distribution* assuming independence of events at $\alpha = 0.05$ level of significance (Bendat and Piersol, 1986). The corresponding t-values are written in parentheses in Table 1 and suggest that significant correlations exist for each category. There are strong relationships between h and other formulations for both and inland stations and for all stability classifications. Coastal stations also perform well for all stability cases except for slightly stable cases where forecasts are not as good along the Gulf coast as they are inland. When ABL height in the model is at its lowest possible value of 50 m, u_* and L are usually small but stability is very high. As a result, examination of extremely stable cases and very stable cases, in Table 1 shows that h_3 is the best approach to the ABL height formulation for the coastal stations BRO, CRP, TLH and TBW. The difference with h_2 is only marginal. The reason for similar correlations between h_1 and h_2 is the strong relationship between u_* and L as explained by Mahrt and Heald (1979). The dependence of u_* on L for each stability category are shown in Figure 3 a, b, c. All correlation values are greater than 0.90 except for the extremely stable case at inland locations.

All stability cases were also considered together for both coastal and inland locations as shown in Figure 3 d, e. Relatively small correlation coefficients between friction velocity and *Monin-Obukhov* length $[r(u_*, L)] = 0.89, 0.70$, were noted, respectively. Figure 3f combines both coastal and inland locations and all stability cases to give a general idea of the results for the locations around the Gulf. In general, the high degree of dependence between u_* and L is evident with a correlation value of 0.82. It is likely that high correlation between u_* and L at coastal locations is due to surface fluxes with heat flux relatively insignificant. Correlation coefficients are somewhat smaller at inland locations because heat flux is more important. It is expected that stability-dependent coefficients (C_m and C_h) used for calculations of heat fluxes (Troen and Mahrt, 1986) will play a significant role to determine wind speed in the ABL during the return-flow cycle. Therefore, with greater stability there will be more wind speed variability in the model.

Table 1. The correlation coefficients (r) between the ABL heights obtained from the model (h) and the ABL heights obtained from the other formulations (h_1, h_2, h_3) for inland and coastal stations around the Gulf of Mexico according to the stability classifications. The number of cases (n) is written for each category, and corresponding *t-values* of the correlation coefficients are given in parentheses. A *t-value* > 1.96 indicates significance at the $\alpha = 0.05$ level assuming independence of events (see text).

Stability and Location	$r(h, H1)$	$r(h, H2)$	$r(h, H3)$
Extremely Stable ($\infty > \mu_* > 78$)			
Coastal n=43	0.74 (6.1)	0.75 (6.2)	0.75 (6.2)
Inland n=19	0.86 (5.2)	0.88 (5.5)	0.88 (5.5)
Very Stable ($78 > \mu_* > 45$)			
Coastal n=53	0.65 (5.5)	0.69 (6.1)	0.70 (6.1)
Inland n=42	0.86 (8.1)	0.88 (8.6)	0.89 (8.9)
Moderately Stable ($45 > \mu_* > 27$)			
Coastal n=45	0.85 (8.1)	0.87 (8.6)	0.87 (8.6)
Inland n=33	0.73 (5.1)	0.78 (5.7)	0.78 (5.7)
Slightly Stable ($27 > \mu_* > 5$)			
Coastal n=29	0.48 (2.7)	0.56 (3.2)	0.57 (3.3)
Inland n=41	0.88 (8.5)	0.82 (7.1)	0.88 (8.5)

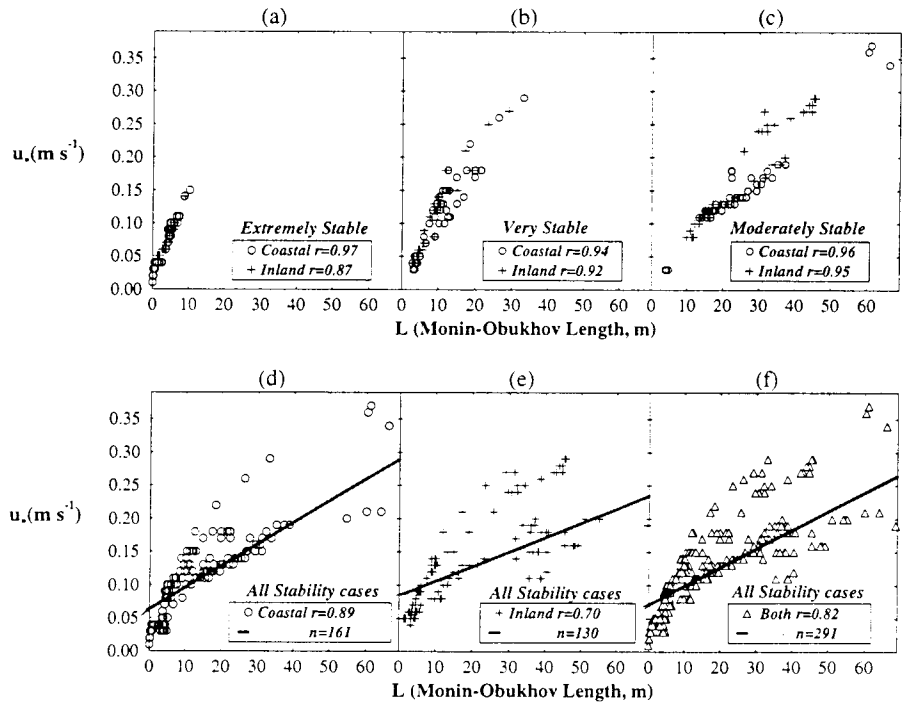

Fig. 3. The dependence of u_* on L for different stability categories (a, b, c) from the OSU model. All stability cases for coastal stations (d) and for inland locations (e) are also indicated. Panel (f) shows the relationship when combining all stability cases and all coastal and inland locations. Solid line indicates an ordinary least squares (OLS) linear regression fit.

3. Stability Dependence on ABL height

Another attempt is made to illustrate the relationship between the stability parameter and ABL heights. Table 2 includes correlation coefficients between both coastal and inland stations. We fail to reject the *null hypothesis* of significant correlations for very stable cases ($78 > \mu_* > 45$) at coastal stations since t-values are less than -1.96. In almost all categories h is well correlated with stability; except for extremely stable cases the relationship between stability and h_3 is very strong.

Table 2. Correlation coefficients (r) between stability parameter (μ_*) and ABL heights (h, h_1, h_2, h_3) using the same stability classifications as in Table 1. The number of cases (n) is written for each category, and corresponding *t-values* of the correlation coefficients are given in parentheses. A *t-value* < -1.96 indicates significance at the $\alpha = 0.05$ level assuming independence of events.

Stability and Location	$r(\mu_*, h)$	$r(\mu_*, H1)$	$r(\mu_*, H2)$	$r(\mu_*, H3)$
Extremely stable				
Coastal n=43	-0.46 (-3.1)	-0.73 (-5.7)	-0.75 (-6.1)	-0.75 (-6.1)
Inland n=19	-0.68 (-3.3)	-0.63 (-2.9)	-0.73 (-3.7)	-0.76 (-4.0)
Very Stable				
Coastal n=53	-0.24 (-1.7)	-0.06 (-0.42)	-0.10 (-0.7)	-0.14 (-0.99)
Inland n=42	-0.56 (-3.9)	-0.36 (-2.3)	-0.47 (-3.2)	-0.49 (-3.3)
Moderately Stable				
Coastal n=45	-0.45 (-3.1)	-0.37 (-2.5)	-0.49 (-3.5)	-0.49 (-3.5)
Inland n=33	-0.59 (-3.7)	-0.24 (-1.3)	-0.40 (-2.3)	-0.40 (-2.3)
Slightly Stable				
Coastal n=29	-0.48 (-2.7)	-0.19 (-0.9)	-0.58 (-3.4)	-0.49 (-2.7)
Inland n=41	-0.56 (-3.9)	-0.42 (-2.8)	-0.78 (-6.4)	-0.73 (-5.7)

The dependence of h on u_* is shown for different stability classifications in Figure 4. This figure clearly shows the nocturnal ABL height is almost linearly related to u_*, especially for the very stable cases with correlation coefficients of 0.82 and 0.86 for coastal and inland locations, respectively. Notice that there is some deviation from linearity for the u_* values greater than 0.2 m s^{-1} at inland locations under moderately stable conditions. In this case large surface fluxes are effective, and it is known that the ABL height is driven by sensible and latent heat fluxes. The dependence of h on u_* is also very similar to that of h on wind speed since wind speed at the surface is well correlated with friction velocity (Koracin and Berkowicz, 1988). The agreement in ABL heights between h and Deardorff's interpolation formula, h_3, can be seen from Figure 4 to be rather good for both coastal and inland locations. It is obvious that especially for the extremely stable and very stable cases, h can be replaced by h_3 to obtain more realistic values (see also Table 1).

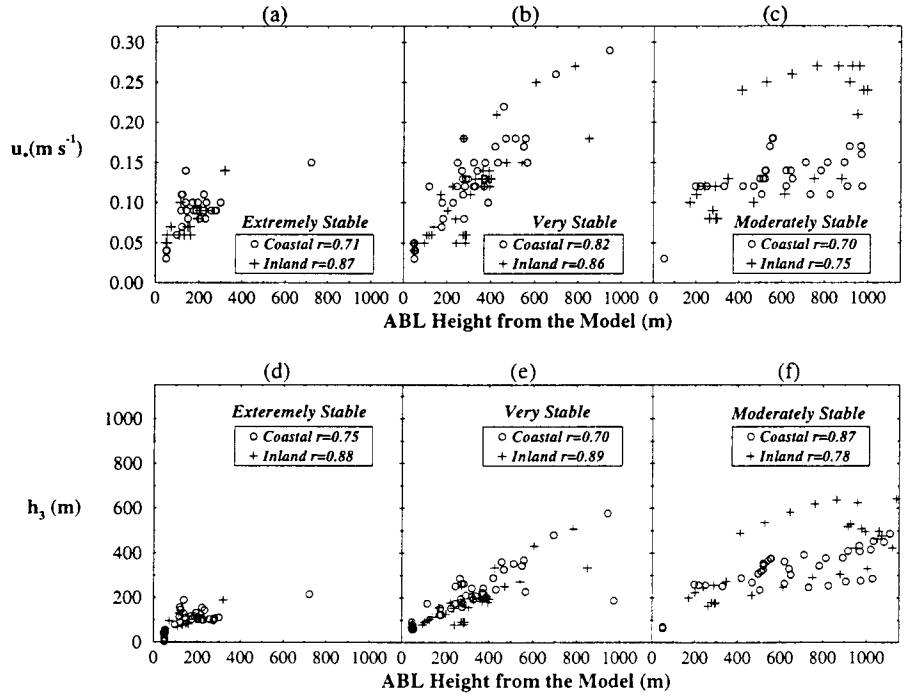

Fig. 4. ABL height from the OSU model formulation (h) versus friction velocity (u_*) including correlation coefficients (r) for both coastal and inland locations. Scatter plots of h vs h_3 are also included for each stability category (d, e, f).

The values of $\frac{f.h}{u_*}$ and $\frac{f.h_3}{u_*}$ are shown as a function of stability parameter (μ_*) in Figure 5 (top 2 panels) to examine if there are any significant tendencies between h and h_3. Frequency distributions of $\frac{f.h}{u_*}$ and $\frac{f.h_3}{u_*}$ are also shown in Figure 5. Here we have a similarity parameter which is useful because it is independent of location and exhibits very small scatter about some decaying exponential function. The similarity hypothesis would also allow the use of μ_* instead of z/L (Zilitinkevich and Deardorff, 1974). In general, coastal and inland locations reflect similar characterictics in terms of the stability parameter ($\mu_* = \frac{k.u_*}{f.L}$). The value of $\frac{f.h_3}{u_*}$ appears to be around 0.2, and an exponential decrease with increasing stability is apparent. On the other hand, the values of $\frac{f.h}{u_*}$ are large in the range, 0.1-0.8 for coastal locations, and the scatter becomes larger under extremely stable conditions. This is probably because of the small values of friction velocity in the boundary layer along the Gulf coast. The frequency distributions shown in Figure 5 indicates that most values are in the range from 0.05 to 0.16 for h_3, and the most likely value is about 0.13. Furthermore, the distributions show that there are no cases when $\frac{f.h_3}{u_*}$ is greater than 0.23 and 0.32 for coastal and inland locations, respectively.

In the same manner the frequency distribution of the ABL height formulation, $\frac{f.h}{u_*}$, is in good agreement with h_3 for smaller values. However, for values greater than approximately 0.3 the results obtained from $\frac{f.h}{u_*}$ do not tend toward zero; in fact, the number of cases of large $\frac{f.h}{u_*}$ is as high as 8. The reason for this difference might be the specification of low level potential temperature, θ^*_{ov}, in the model (Kara *et al.*, 1997). This term ignores surface heat flux during night, and it has some influence on the ABL height determination, especially under very stable conditions.

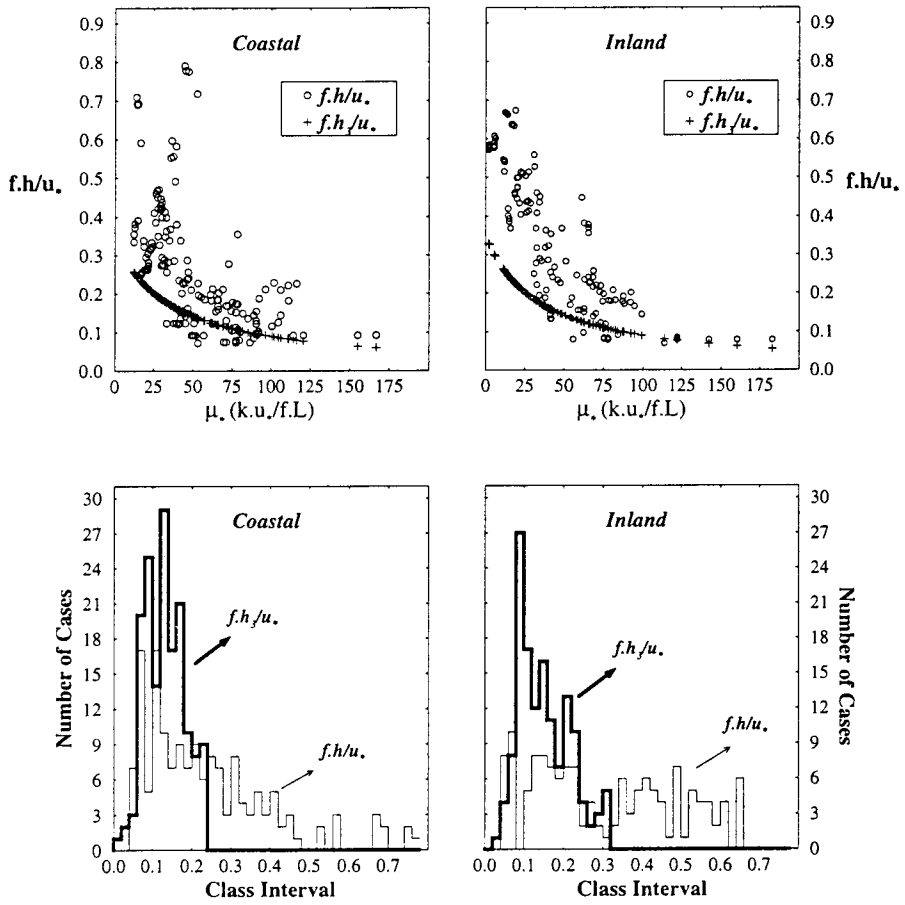

Fig. 5. Dependence of $(f.h/u_*)$ and $(f.h_3/u_*)$ on stability parameter (μ_*) at both coastal and inland locations (top 2 panels). Frequency distributions of these two cases, $f.h/u_*$ (thin line) and $f.h_3/u_*$ are also shown with a class interval of 0.02.

4. Temperature Structure Parameter

We have also examined BRO, JAN, and TBW to determine the dependence of geostrophic wind on the structure parameter. The stability parameter z/L is examined for determination of the structure parameter. We have used the structure parameter of temperature in dimensionless form in terms of the z/L, following Sorbjan (1986) as shown below:

$$CTN = 3.2\frac{[5h/L.z/h + (1-z/h)^{1.5\alpha_1-\alpha_2}]}{[4h/L.z/h + (1-z/h)^{1.5\alpha_1-\alpha_2}]^{1/3}}\ \frac{(1-z/h)^{8/(3\alpha_2-2\alpha_1)}}{(z/h)^{2/3}} \tag{5}$$

where, $\alpha_1 = \alpha_2$ is taken as 1 for simplicity, and they depend on terrain slope (Lacser and Arya, 1986). We examine the vertical profiles of the structure parameter of temperature using h and L obtained from the ABL model forecasts for coastal and inland locations during a return-flow cycle. Since the model of Nieuwstadt (1984) does not describe the profile of the structure parameter, we used Sorbjan's definition (Cuijpers and Kohsiek, 1988). In Sorbjan's formulation the profile of the structure parameter in the surface layer is well described but it is highly dependent on the values of α_1 and α_2 above the surface layer.

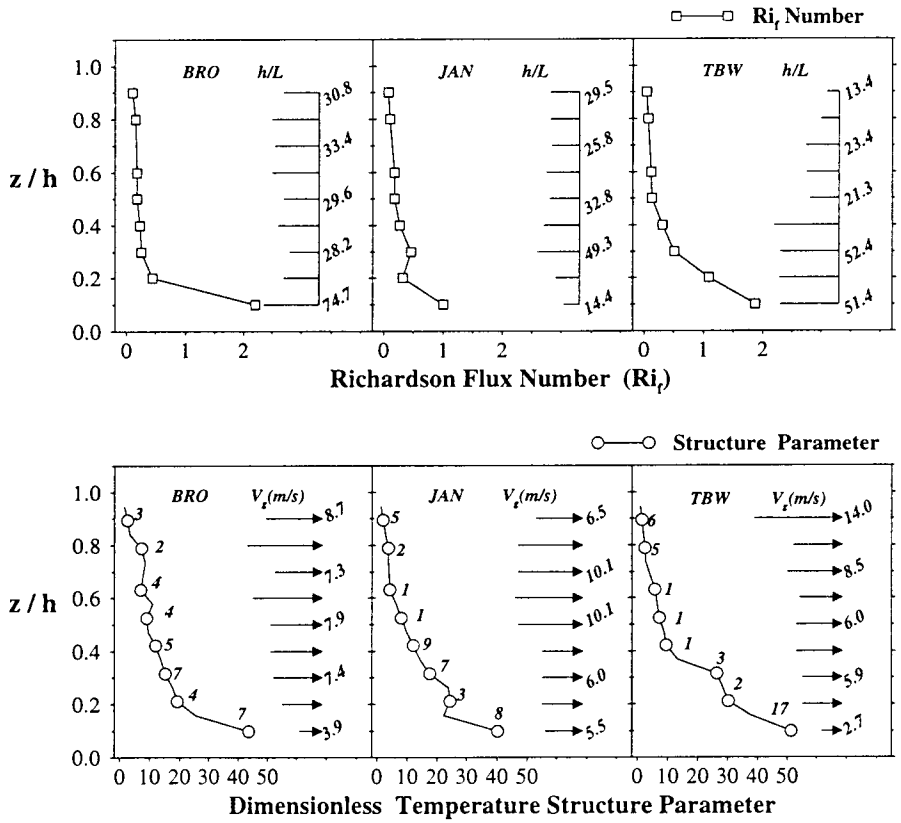

Fig. 6. The average of Richardson flux number (Ri_f) as a function of height at every 100 m and calculated profiles of the dimensionless temperature structure parameter for different values of the stability at 100 m intervals for BRO, JAN and TBW during nights of Feb 2-9 return-flow cycle. The numbers on the structure parameter plots represent data points within each height interval over which calculations were performed, and the average value of structure parameter at each 100 m interval is represented by a small circle. Selected h/L and geostrophic wind (V_g) values at 200 m intervals are also included. The length of each line shows the magnitude of h/L and wind speed (m s^{-1}).

The Richardson flux numbers (Ri_f) as a function of ABL height for BRO, JAN and TBW are shown in Figure 6. The values of h/L are also written at each level. Calculations were performed by using the model forecasts obtained 4 hours after sunset to avoid the transition period during which turbulence is dominated by nonstationary effects. As can be noticed from Figure 6, Richardson flux values at the surface are large at two coastal stations, BRO and TBW, compared with JAN. Above the surface layer Richardson flux number is almost constant except for TBW which shows a gradual decrease of Ri_f with height below 300 m.

The vertical profiles of the dimensionless temperature parameter are also shown in Figure 6 (bottom 3 panels). Wind speeds at selected levels are included for each station in the panels. The length of each arrow shows the magnitude of wind speed at that level. The *Monin- Obukhov* lengths were averaged at each 100 m and used for the calculations of the structure parameter at each 100 m height interval. The ABL collapsed most frequently at TBW during the return-flow event, and this can be noticed by examining the number of data points (n = 17) over which calculations were performed at the surface. Increasing values of structure parameter are noted near the surface, and small values are found at the top of the ABL. Interestingly, the structure parameter extends to a value as high as 50 in the surface boundary layer at TBW. On the other hand, BRO and JAN show almost similar characteristics in terms of the structure parameter.

We also noticed that although Ri_f values are almost the same for BRO and TBW at the surface, the structure parameter is larger at TBW than at BRO. This is probably due to the effect of mechanical turbulence. In the model, winds are often light at TBW, and mechanical turbulence would cause the temperature parameter to be large at the surface. Shear turbulence would be expected at BRO because of stronger winds. Even though JAN has a small value of the temperature structure parameter in comparison with BRO and TBW when z/h is 0.14 at JAN, the wind is as strong as 5.5 m s^{-1}, indicating the delayed effect of moisture increase at inland locations during the return-flow.

5. Conclusions

The model performance in predicting atmospheric boundary layer parameters, particularly the ABL height, friction velocity (u_*), *Monin-Obukhov* (L) lengths and temperature structure parameter (CTN), were examined for the U. S. coastal and inland stations around the Gulf of Mexico during a single return-flow event. The agreement in ABL heights between h and Deardorff's interpolation formula, h_3, was found to be rather good for both coastal and inland locations. Therefore, the ABL height formulation in the model can be replaced by an interpolation formula to obtain more realistic values under very stable conditions at night. Correlation coefficients showed that the friction velocity is highly dependent on L in the model formulation. This relationship between u_* and L at coastal locations is due to surface fluxes. Correlation coefficients are relatively small at inland locations because heat flux is more important. Since stability-dependent coefficients play a significant role in the determination of wind speed in the ABL during the return-flow event, the greater the stability the more variability of model wind speed. We also found the values of $\frac{f.h}{u_*}$ are large, between 0.1-0.8 for coastal locations, and the scatter becomes larger under extremely stable conditions. This is probably due to the small values of friction velocity within the surface ABL along the Gulf coast. Examination of the temperature structure parameter indicated mechanical turbulence would cause the temperature parameter to be large at the surface since wind speeds were not predicted to be very strong in the model for the coastal location of Tampa Bay (TBW), Florida. Examination of other return-flow events will provide insight into whether or not all these results generalize.

Acknowledgements

We would like to thank Dr. Paul H. Ruscher of Florida State University for allowing us to extend his research under contract number F19628-93-K-0006 by the U. S Air Force of Scientific Research. Dr. John Lewis of the National Severe Storm Laboratory is thanked for his helpful comments about return-flow events over the Gulf of Mexico. Our thanks also go to Matt Carter of the Florida State University for helping us to extract many upper-air sounding files from NCAR data archieve. We would like to thank reviewers for their helpful comments. Partial financial support for this work came from NOAA through the Cooperative Institute on Tropical Meteorology.

REFERENCES

André, J. C., and L. Mahrt, 1982. The nocturnal surface inversion and influence of clear air radiative cooling. *J. Atmos. Sci.* **39**, 864-878.

Bendat, J. S., and A. G. Piersol, 1986. *Random Data.* Wiley, 566 pp.

Benkley, C. W., and L. Schulman, 1979. Estimating hourly mixing depths from historical meteorological data. *J. Appl. Meteor.*, **18**, 772-780.

Businger, J. A., and S. P. S. Arya, 1974. Heights of the mixed layer in the stably stratified planetary boundary layer. *Adv. Geophys.*, **18A**, Academic Press, 73-92.

Clarke, R. H., 1970. Observational studies in the atmospheric boundary layer. *Quart. J. Roy. Meteor. Soc.*, **96**, 91-114.

Clarke, R.H., and G. D. Hess, 1973. On the appropriate scaling for velocity and temperature in the planetary boundary layer. *J. Atmos. Sci.*, **30**, 1346-1353.

Crisp, C. A., and J. M. Lewis, 1992. Return-flow in the Gulf of Mexico. Part I: A classificatory approach with a global historical perspective. *J. Appl. Meteor.*, **31**, 868-881.

Cuijpers, J. W., and W. Kohsiek, 1988. Vertical profiles of the structure parameter of temperature in the stable, nocturnal boundary layer. *Bound. -Layer Meteor.*, **47**, 111-129.

Deardorff, J. W., 1972. Parameterization of the planetary boundary layer for use in general circulation models. *Mon. Wea. Rev.*, **100**, 93-106.

Kara, A. B., 1996. Analysis of boundary layer structure over and around the Gulf of Mexico. Master thesis, Department of Meteorology, The Florida State University, 78 pp.

Kara, A. B., J. B. Elsner, and P. H. Ruscher, 1997. Physical Mechanism for the Tallahassee, FL minimum temperature anomaly. *J. Appl. Meteor.*, **37**, 101-113.

Kara, A. B., P. H. Ruscher, and J. B. Elsner, 1998. Numerical models of boundary layer processes over and around the Gulf of Mexico during a return-flow event. In press *Wea. Forecasting*, December issue.

Koracin, D., and R. Berkowicz, 1988. Nocturnal boundary layer height. Observations by acoustic sounders and predictions in terms of surface layer parameters. *Bound. -Layer Meteor.*, **43**, 65-83.

Lacser, A., and S. P. S. Arya, 1986. A numerical model study of structure and similarity scaling of the nocturnal boundary layer. *Bound. -Layer Meteor.*, **35**, 369-385.

Lewis, J. M., and A. C. Crisp, 1992. Return-flow in the Gulf of Mexico. Part II: Variability in return-flow thermodynamics inferred from trajectories over the Gulf. *J. Appl. Meteor.*, **31**, 868-881.

Mahrt, L., and R. C. Heald, 1979. Comments on "Determining height of the nocturnal boundary layer". *J. Appl. Meteor.*, **36**, 383.

Mahrt, L., and H. -L. Pan, 1984. A two-layer model of soil hydrology. *Bound. -Layer Meteor.*, **29**, 1-20.

Nieuwstadt, F. T. M., 1984. The turbulent structure of the stable, nocturnal boundary layer. *J. Atmos. Sci.*, **41**, 2202-2216.

Pan, H. -L, and L. Mahrt, 1987. Interaction between soil hydrology and boundary layer development. *Bound. -Layer Meteor.*, **38**, 185-202.

Ruscher, P. H., 1988. Parameterization of the very stable boundary layer in a simple model. *Proc. 8th Symp. Turb. Diff.*, San Diego, CA, Amer. Meteor. Soc., 299-301.

Sorbjan, Z., 1986. On similarity in the atmospheric boundary layer. *Bound. -Layer Meteor.*, **34**, 377-397.

Troen, I., and L. Mahrt, 1986. A simple model of the atmospheric boundary layer model. Sensitivity to surface evaporation. *Bound. -Layer Meteor.*, **37**, 129-148.

Yu, T-W., 1977. Determining the height of the nocturnal boundary layer. *J. Atmos. Sci.*, **17**, 28-33.

Zhang, D., and R. A. Anthes, 1982. A high resolution model of the planetary boundary layer model- Sensitivity tests and comparisons with SESAME-70 data. *J. Appl. Meteor.*, **21**, 1594-1609.

Zilitinkevich, S. S., and J. W. Deardorff, 1974. Similarity theory for the planetary boundary layer of time-dependent height. *J. Atmos. Sci.*, **31**, 1449-1452.